



**ELECTROCHEMICAL CHARACTERIZATION OF $\text{La}_{0.6}\text{Sr}_{0.4}\text{CoO}_3$
AND $\text{La}_{0.6}\text{Sr}_{0.4}\text{CoO}_3$ DOPED WITH RuO_2 POWDERS AS THE NEXT
GENERATION SUPERCAPACITORS**

**Miroslav M. Pavlovic^{1*}, S. Erakovic¹, V. Panic¹, M. R. Pantovic Pavlovic¹,
S. Stopic², B. Friedrich²**

¹ICTM, DEC, University of Belgrade, Njegoseva 12, Belgrade, SERBIA

²IME Process Metallurgy and Metal Recycling; RWTH Aachen University,
Aachen, GERMANY

*mpavlovic@tmf.bg.ac.rs

ABSTRACT

In this study, $\text{La}_{0.6}\text{Sr}_{0.4}\text{CoO}_3$ (LSC) powder and LSC doped with 20 wt.% RuO_2 were investigated as anode materials for supercapacitor. Spherical submicron particles of $\text{La}_{0.6}\text{Sr}_{0.4}\text{CoO}_3$ have been synthesized by ultrasonic spray pyrolysis. Morphology of LSC powder was examined by scanning electron microscopy coupled with energy-dispersive X-ray spectroscopy. Both powders were examined by X-ray diffraction, which indicated that substitution of Ru for Sr and Co in the base strongly increased the electrocatalytic activity of the oxide. Electrochemical characterization results have shown improvement in capacitive characteristics of doped LSC showing that this material is good prerequisite for supercapacitor.

Key words: perovskite oxide, supercapacitor, cyclic voltammetry, ultrasonic spray pyrolysis.

INTRODUCTION

Nowadays, the development of high energy supercapacitors has received considerable attention worldwide. Supercapacitors, as a new promising energy storage device, are electrochemical energy storage devices that play an important role in energy storage and delivery. They have many advantages such as faster charging/discharging rate, long idle life cycle, higher power energy density and green environmental protection compared to other chemical energy storage devices [1-4]. The boundary of energy and power density of supercapacitors existing between high power electric capacitors and high energy fuel cells can be determined in the Ragone plot.

However, the previous supercapacitors suffer from low energy density [1, 5, 6]. Hence, in order to meet the development of supercapacitors, their energy density should be substantially enhanced without deteriorating their high power capability and cycle life [7]. Since the active materials in electrodes of supercapacitor determine its electrochemical performance and energy storage capacity a lot, numerous new materials have been widely designed and prepared [8, 9]. It is well-known that the performance of

supercapacitors is strongly determined by the properties and structures of electrode materials [10]. Thus, many efforts have been made to design and prepare the electrodes of supercapacitors.

Most popular materials today are particle materials, which have high surface areas for charge storage [11, 12]. Among them, transition metal oxides (TMOs) are considered as ideal electrode materials for supercapacitors as they can provide both a high specific capacitance and a high energy density. A promising candidate for application is strontium substituted lanthanum cobalt oxide $\text{La}_{0.6}\text{Sr}_{0.4}\text{CoO}_3$, a perovskite-type material with a mixed ionic and electronic conductivity (MIEC) at elevated temperatures [13]. Perovskite oxide (ABO_3) displays both good oxygen ion and electron conductivity which could provide some oxygen vacancies to enhance the transfer of oxygen ion. These characteristics make them become excellent cathode materials of solid oxide fuel cell and the potential substitution of bifunctional catalyst compared with precious metal catalyst in Li-air batteries [14]. Perovskites have been paid much attention in past decades because of their stable structure, high-temperature sustainability, catalytic property, and crucial role in solid fuel cells and solar cells [15].

The spray-pyrolysis method was applied for synthesis of the starting powders of the cathode ($\text{La}_{0.6}\text{Sr}_{0.4}\text{CoO}_3$) and anode (a samaria-doped ceria-NiO composite powder). In this study, different microstructures of the cathode were obtained by varying the sintering temperature from 950 to 1200 °C [16].

La-doped SrTiO_3 (LST) powders were prepared by ultrasonic spray pyrolysis using an aqueous solution of a metal nitrate [17]. SEM images showed that the as-prepared LST powders had a spherical morphology with a diameter of 1 μm . XRD patterns showed that the crystal phase of the as-prepared powders was amorphous and that the powders crystallized to the perovskite phase by calcination at 900 °C. The sintered LST body had the highest electrical conductivity at a La doping concentration (La_x) of 0.1 under a reducing atmosphere.

The material characterization techniques were implemented to acquire the crystallinity, surface area, and porosity. Consequently, the good electrochemical response was obtained from cyclic voltammetry (CV) studies. The as-prepared samples clearly revealed that the perovskite materials are promising candidate for supercapacitor electrode materials. The aim of this work is synthesis and characterization of submicron particles of $\text{La}_{0.6}\text{Sr}_{0.4}\text{CoO}_3$ prepared by ultrasonic spray pyrolysis in one single step.

EXPERIMENTAL

Material synthesis - preparation of LSC and LSC w / 20 wt. % RuO_2 nanoparticles

Lanthanum nitrate, strontium nitrate, cobalt nitrate were used as precursor for the synthesis of $\text{La}_{0.6}\text{Sr}_{0.4}\text{CoO}_3$ submicron by ultrasonic spray pyrolysis. The temperature and pressure control was adjusted using a thermostat and a vacuum pump. Atomization of the obtained solution after dissolution of precursor took place in an ultrasonic atomizer (Gapusol 9001, RBI/France) with one transducer to create the aerosol. The resonant frequency was selected to be 2.5 MHz. The concentration of nitrogen was

flushed from bottle to remove air from the system. Under spray pyrolysis conditions, nitrogen overpassed continuously through the quartz tube (at a flow rate of the 3 l/min). Then atomized droplets were further transported by carrier gas to the vertical furnace, company Thermostar, Aachen. After thermal decomposition of transported aerosol in the furnace, the formed nanopowder of $\text{La}_{0.6}\text{Sr}_{0.4}\text{CoO}_3$ was collected with an electrostatic precipitator.

The precursor solution was investigated in water and alkaline solution. It was concluded that the LSC powder was stable both in aqueous and alkaline solutions. Therefore, the process of preparing $\text{La}_{0.6}\text{Sr}_{0.4}\text{CoO}_3$ powder doped with 20 wt. % RuO_2 was firstly suspending LSC in deionized water in ultrasonic bath for 30 min. Afterwards, 40 μl of 0.1 M KOH was added to adjust pH value from 8.1 to 10. After in the mixture that was continuously stirred the 661 μl of RuCl_3 solution was added and pH value was adjusted with 100 μl 0.1 M KOH to 8.5.

Characterization

SEM and EDS analysis of strontium substituted lanthanum cobalt oxide $\text{La}_{0.6}\text{Sr}_{0.4}\text{CoO}_3$, a perovskite-type material were performed using scanning electron microscope VEGA TS 5130MM microscope (Tescan).

Phase analysis was examined by X-ray diffraction (XRD) measurements on Philips PW 1050 powder diffractometer at room temperature with Ni filtered $\text{CuK}\alpha$ radiation ($\lambda = 1.54178 \text{ \AA}$) and scintillation detector within $10\text{--}82^\circ$ 2θ range in steps of 0.05° , and scanning time of 5 s per step.

Electrochemical measurements were performed in a three-electrode cell. For this purpose, an electrochemical work station (BioLogic, SP-240) having potentiostat/galvanostat provided with corrosion and physical electrochemistry software and a desktop computer (HP) was used. A platinum foil and $\text{Hg/HgO}/1\text{M KOH}$ electrode ($E^\circ = 0.098 \text{ V vs NHE at } 25^\circ\text{C}$) were used as counter and reference electrode, respectively. The working electrode geometric area exposed to electrolyte was 0.39 cm^2 . The cell was filled with 0.1 M KOH electrolyte and purged with N_2 for 30 min prior to and continuously during electrochemical measurements.

RESULTS AND DISCUSSION

Scanning electron microscopy

Morphology of the perovskite $\text{La}_{0.6}\text{Sr}_{0.4}\text{CoO}_3$ (LSC) powder was examined by scanning electron-microscopy. SEM photographs of the powder used as supercapacitor before doping with RuO_2 and before dissolution in KOH are shown in Figure 1a, while morphology of the perovskite $\text{La}_{0.6}\text{Sr}_{0.4}\text{CoO}_3$ powder after immersion in 0.1M KOH solution and consequent drying in inert N_2 atmosphere at 150°C for 3 h is shown on Figure 1b.

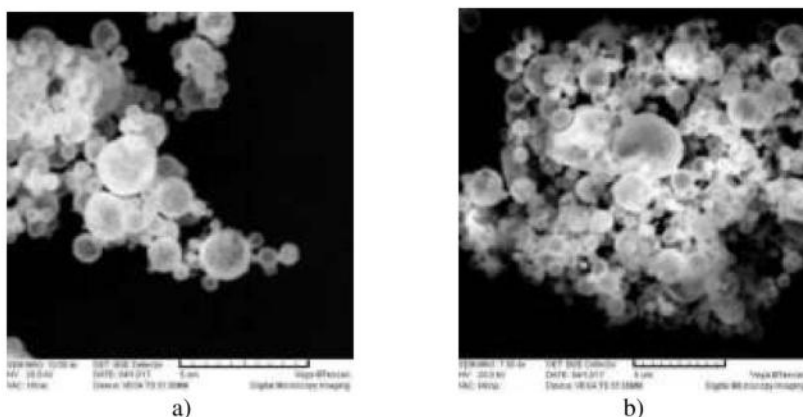


Figure 1. SEM micrographs of perovskite $\text{La}_{0.6}\text{Sr}_{0.4}\text{CoO}_3$ powder a) before and b) after immersing in 0.1M KOH solution and consequent drying. Magnification a) x10K and b) x7K

As it can be seen, LSC oxide is stable in alkaline solution, with unchanged morphology. Results of SEM micrographs show that material used is in the form fine rounded powder with powder particles ranging from 0.5-4.5 μm . Figure indicates that features of each oxide powder is more or less similar in nature and that it has definite regular structure.

Elemental analysis of the each oxide has been carried out by EDS analysis, and the results, so obtained, are shown in Figures 2 and 3.

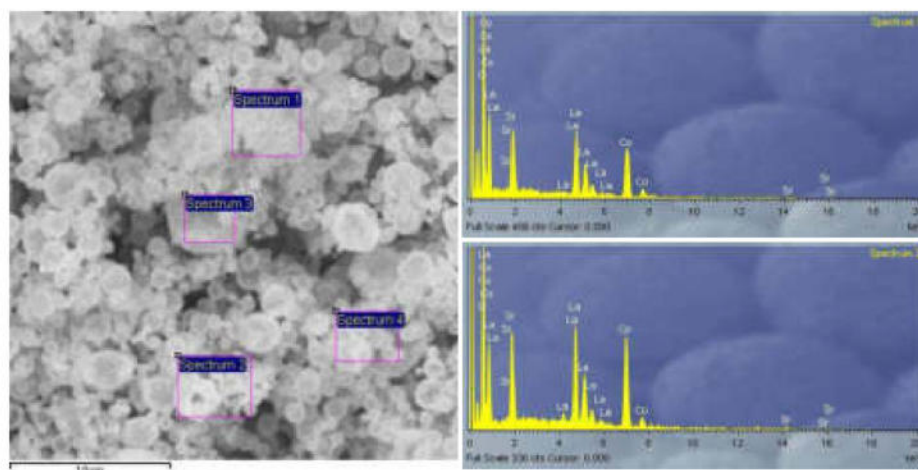


Figure 2. EDS analysis of used LSC oxide with spectrum analysis of site 1 (top) and site 2 (bottom)

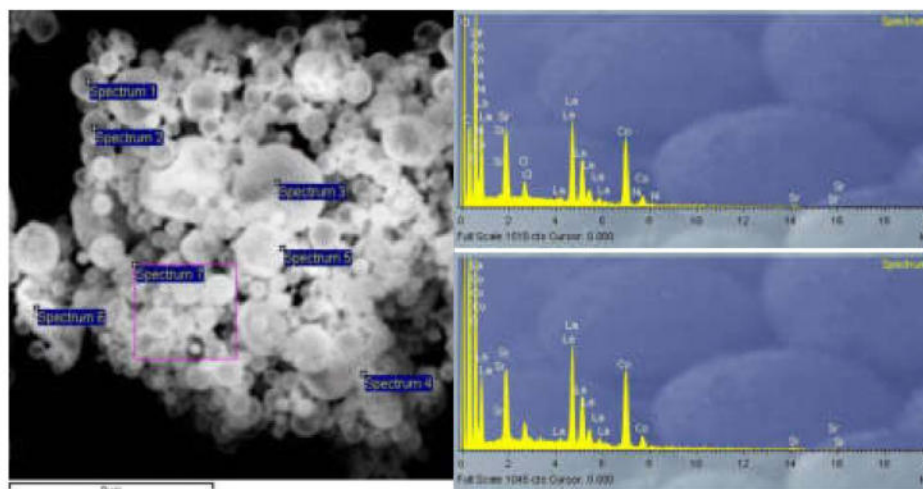


Figure 3. EDS analysis of used LSC oxide after immersion in 0.1 M KOH with spectrum analysis of site 1 (top) and site 7 (bottom)

Table 1 and 2 show atomic % of each element at examined sites. As it can be seen, comparing results from both tables, there is no dissolution of any element in KOH, i.e. the LSC powder is stable in alkaline solution.

Table 1. Elemental analysis of used LSC powder at examined sites

Spectrum	Co	Sr	La	O
Spectrum 1	22.73	9.56	14.17	53.54
Spectrum 2	24.17	8.22	14.09	53.52

Table 2. Elemental analysis of LSC powder immersed in KOH at examined sites

Spectrum	Co	Sr	La	O
Spectrum 1	23.29	9.42	13.83	53.46
Spectrum 7	23.95	7.89	14.53	53.63

X-ray diffraction analysis

XRD patterns for two powders ultrasonically synthesized e.g. lanthanum strontium cobalt oxide ($\text{La}_{0.6}\text{Sr}_{0.4}\text{CoO}_3$) and LSC doped with 20 wt. % RuO_2 are represented in Figure 3.

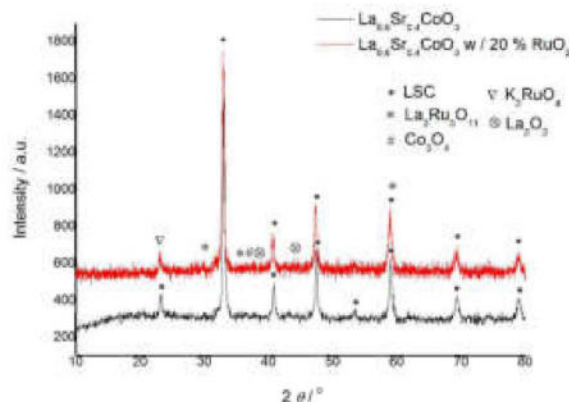


Figure 4. XRD patterns for LSC and doped LSC powders produced by ultrasonic spray pyrolysis

Figure 4 shows the XRD patterns of the as-fabricated sample and powder doped with ruthenium oxide. By comparing the results with XRD pattern (JCPDS PDFNo. 01-89-2528) of the standard $\text{La}_{0.6}\text{Sr}_{0.4}\text{CoO}_3$ sample, it can be seen that all of the XRD peaks of each sample in the 2θ range of $10\text{--}80^\circ$ could be well indexed, as shown in Figure 4. In other words, the LSC powder was of single-phase with rhombohedral crystal structure. For perovskite, as well as other crystalline materials, the variation in the crystal structure may lead to distinct electrocatalytic activities [18]. It was found that LSC has identical rhombohedral lattice which can be indexed according to R-3c space group symmetry (#161). This fact rules out the significant effect that crystal structure may have on the activities [18]. However, new diffraction peaks can be distinguished after doping with 20 wt. % of RuO_2 due to the presence of new Co_3O_4 , La_2O_3 , $\text{La}_3\text{Ru}_3\text{O}_{11}$ and K_2RuO_4 phases, indicating that the new nanoparticle (NP) compounds were highly dispersed on the LSC surface.

An unknown weak peak at around $2\theta=38^\circ$ was attributed to lanthanum oxide, La_2O_3 , according to the JCPDS PDFNo. 00-40-1279 XRD database, which was considered to be the result of a partial decomposition of the LSC [19]. In addition, the diffraction signals assignable to the $\text{La}_3\text{Ru}_3\text{O}_{11}$ and K_2RuO_4 (JCPDS PDF No.01-070-1086 and 01-051-1751, respectively) phase became apparently detected in doped samples, indicating the formation of small amount of ruthenium compound with lanthanum and potassium. Figure 4 also shows the typical XRD peak of the obtained Co_3O_4 in which all the diffraction could be indexed as the cubic Co_3O_4 spinel phase (JCPDS PDF No. 01-078-1969) [20].

Electrochemical analysis

The cyclic voltammograms of LSC and LSC doped with RuO_2 on glassy carbon (GC) substrate were recorded at the scan rate of 20 mV s^{-1} in the potential region $-0.2\text{--}0.5$

V in 0.1 M KOH, at room temperature. A representative curves for each sample are shown in Figure 5. Upon exposure of the GC electrode with LSC and LSC doped with 20 wt. % RuO_2 to potentiodynamic changes, a stable capacitive CV response was registered, in a potential window as wide as 0.7 V in the case of LSC with 20 wt. % RuO_2 .

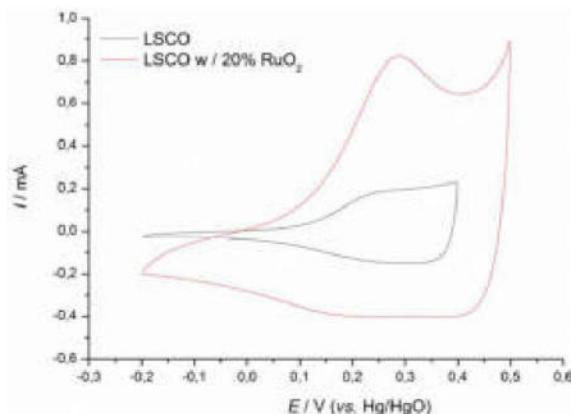


Figure 5. Cyclic voltammograms at a scan rate of 20 mV/s for LSC and LSC doped with RuO_2 at room temperature

The shape of the CV curve of the LSC powder is different with respect to that registered for the LSC powder doped with 20 wt. % of RuO_2 . One well-separated peak for the LSC with 20 wt. % of RuO_2 coating at around 0.29 V is seen. The Figure 5 showed that voltammograms of the oxide electrode exhibited a pair of redox peaks, one anodic ($E_{pa} = 290\text{mV}$) and a corresponding broad cathodic peak ($E_{pc} = 150\text{mV}$), prior to the onset of oxygen evolution reaction.

The capacitance of LSC was considerably lower, which indicates poor conductivity in the cathodic direction. An LSC powder doped with 20 wt. % of RuO_2 exhibits a considerable increase in the voltammetric capacitance, due to pronounced ruthenium injection into crystal structure of LSC.

CONCLUSION

Capacitive properties of LSC colloidal dispersion and the effects of doping LSC with ruthenium oxide were investigated. SEM-EDS analyses show that LSC material is in the form of fine rounded powder stable in both aqueous and alkaline solutions. The X-ray diffraction study indicated the formation of pure perovskite phase of the material with rhombohedral crystal geometry. The substitution of Ru for Sr and Co in the base strongly increased the electrocatalytic activity of the oxide and the value being highest with 20 wt. % ruthenium oxide. CV studies of the Ru doped LSC material indicate improvement in capacitive response of the material, exhibiting that this material is good prerequisite for supercapacitor. The activity of this oxide is several times higher than the one observed by LSC.

Acknowledgement

This work was financially supported by Ministry of Education, Science and Technological Development of the Republic of Serbia under the research projects: ON172037, ON172046 and ON172060.

REFERENCES

1. Cao, Y.; Lin, B.; Sun, Y.; Yang, H.; Zhang, X., Sr-doped Lanthanum Nickellate Nanofibers for High Energy Density Supercapacitors. *Electrochimica Acta*, 174, 41-50, 2015.
2. Arjun, N.; Pan, G.-T.; Yang, T. C. K., The exploration of Lanthanum based perovskites and their complementary electrolytes for the supercapacitor applications. *Results in Physics*, 7, 920-926, 2017.
3. Pan, H.; Li, J.; Feng, Y., Carbon Nanotubes for Supercapacitor. *Nanoscale Research Letters*, 5, (3), 654, 2010.
4. Yang, Y.; Zhang, H.; Zhu, G.; Lee, S.; Lin, Z.-H.; Wang, Z. L., Flexible Hybrid Energy Cell for Simultaneously Harvesting Thermal, Mechanical, and Solar Energies. *ACS Nano*, 7, (1), 785-790, 2013.
5. Yuan, C.; Yang, L.; Hou, L.; Shen, L.; Zhang, X.; Lou, X. W., Growth of ultrathin mesoporous Co₃O₄ nanosheet arrays on Ni foam for high-performance electrochemical capacitors. *Energy & Environmental Science*, 5, (7), 7883-7887, 2012.
6. Snook, G. A.; Kao, P.; Best, A. S., Conducting-polymer-based supercapacitor devices and electrodes. *Journal of Power Sources*, 196, (1), 1-12, 2011.
7. Wang, F.; Xiao, S.; Hou, Y.; Hu, C.; Liu, L.; Wu, Y., Electrode materials for aqueous asymmetric supercapacitors. *RSC Advances*, 3, (32), 13059-13084, 2013.
8. Wang, G.; Xu, H.; Lu, L.; Zhao, H., One-step synthesis of mesoporous MnO₂/carbon sphere composites for asymmetric electrochemical capacitors. *Journal of Materials Chemistry A*, 3, (3), 1127-1132, 2015.
9. Zhang, D.; Yan, H.; Lu, Y.; Qiu, K.; Wang, C.; Zhang, Y.; Liu, X.; Luo, J.; Luo, Y., NiCo₂O₄ nanostructure materials: morphology control and electrochemical energy storage. *Dalton Transactions*, 43, (42), 15887-15897, 2014.
10. Luo, L.; Liu, T.; Zhang, S.; Ke, B.; Yu, L.; Hussain, S.; Lin, L., Hierarchical Co₃O₄@ZnWO₄ core/shell nanostructures on nickel foam: Synthesis and electrochemical performance for supercapacitors. *Ceramics International*, 43, (6), 5095-5101, 2017.
11. Abdur, R.; Kim, K.; Kim, J.-H.; Lee, J., Electrochemical behavior of manganese oxides on flexible substrates for thin film supercapacitors. *Electrochimica Acta*, 153, 184-189, 2015.
12. Kazemi, S. H.; Asghari, A.; kiani, M. A., High Performance Supercapacitors Based on the Electrodeposited Co₃O₄ Nanoflakes on Electro-etched Carbon Fibers. *Electrochimica Acta*, 138, 9-14, 2014.

13. Hayd, J.; Dieterle, L.; Guntow, U.; Gerthsen, D.; Ivers-Tiffée, E., Nanoscaled $\text{La}_{0.6}\text{Sr}_{0.4}\text{CoO}_{3-\delta}$ as intermediate temperature solid oxide fuel cell cathode: Microstructure and electrochemical performance. *Journal of Power Sources*, 196, (17), 7263-7270, 2011.
14. Sun, N.; Liu, H.; Yu, Z.; Zheng, Z.; Shao, C., The $\text{La}_{0.6}\text{Sr}_{0.4}\text{CoO}_3$ perovskite catalyst for Li-O₂ battery. *Solid State Ionics*, 268, Part A, 125-130, 2014.
15. Zhu, J.; Li, H.; Zhong, L.; Xiao, P.; Xu, X.; Yang, X.; Zhao, Z.; Li, J., Perovskite Oxides: Preparation, Characterizations, and Applications in Heterogeneous Catalysis. *ACS Catalysis*, 4, (9), 2917-2940, 2014.
16. Maric, R.; Ohara, S.; Fukui, T.; Yoshida, H.; Nishimura, M.; Inagaki, T.; Miura, K., Solid Oxide Fuel Cells with Doped Lanthanum Gallate Electrolyte and LaSrCoO_3 Cathode, and Ni-Samarium-Doped Ceria Cermet Anode. *Journal of The Electrochemical Society*, 146, (6), 2006-2010, 1999.
17. Genji, K.; Myoujin, K.; Kadera, T.; Ogihara, T., Synthesis and Electrical Properties of La Doped SrTiO_3 Powders by Ultrasonic Spray Pyrolysis. *Key Engineering Materials*, 582, (9), 115-118, 2013.
18. He, J.; Sunarso, J.; Zhu, Y.; Zhong, Y.; Miao, J.; Zhou, W.; Shao, Z., High-performance non-enzymatic perovskite sensor for hydrogen peroxide and glucose electrochemical detection. *Sensors and Actuators B: Chemical*, 244, 482-491, 2017.
19. Park, J.-S.; Chung, W.-H.; Kim, H.-S.; Kim, Y.-B., Rapid fabrication of chemical-solution-deposited $\text{La}_{0.6}\text{Sr}_{0.4}\text{CoO}_{3-\delta}$ thin films via flashlight sintering. *Journal of Alloys and Compounds*, 696, 102-108, 2017.
20. Che, H.; Lv, Y.; Liu, A.; Mu, J.; Zhang, X.; Bai, Y., Facile synthesis of three dimensional flower-like $\text{Co}_3\text{O}_4@\text{MnO}_2$ core-shell microspheres as high-performance electrode materials for supercapacitors. *Ceramics International*, 43, (8), 6054-6062, 2017.